Geomechanics and Engineering, *Vol. 31, No. 6 (2022) 615-622*
https://doi.org/10.12989/gae.2022.31.6.615

Wave propagation in an FG circular plate in thermal environment

Gui-Lin She* and Yin-Ping Li

College of Mechanical and Vehicle Engineering, Chongqing University, Chongqing 400044, China

(*Received October 7, 2021, Revised November 27, 2022, Accepted December 15, 2022*)

Abstract. In this paper, considering the temperature dependence of material physical parameters as well as the effects of thermal effect and shear deformation, we have conducted an in-depth study on the wave propagation of functionally graded (FG) materials circular plate in thermal environment based on the physical neutral surface concept. The dynamic governing equations of functionally graded plates are established, and the dispersion relation of wave propagation is derived. The influence of different temperature fields on the propagation characteristics of flexural waves in FG circular plates is discussed in detail. It can be found that the phase velocity and group velocity of wave propagation in the plate decrease with the increase of temperature.

Keywords: circular plate; FG materials; physical neutral surface concept; porosities; wave propagation

1. Introduction

When the ambient temperature changes, the whole structure or each part will shrink and expand with the increase or decrease of temperature. This kind of external factors that cause the change of structure temperature field is temperature load. As a kind of basic structure, the circular plate structure is widely used in engineering practice. Under the action of various loads, different geometric parameters and boundary conditions will produce different dynamic responses to the plate structure. If the change of ambient temperature is further considered, its response will become more complex. The temperature field will cause the circular plate structure to produce temperature stress, which will affect the vibration characteristics of the plate structure. For the circular plate, the change of its surrounding temperature will cause obvious temperature stress in the circular plate, which will cause the beam to produce temperature stress and strain. In structural design, temperature effect is inevitable. Therefore, it is very meaningful to study the wave propagation of circular plate structures in thermal environment.

The main physical parameters of functionally graded (FG) materials often change uniformly along the thickness direction (Zenkour and Radwan 2019, Dehrouyeh-Semnani *et al.* 2019, Ahmadi 2019, Akgoz and Civalek 2017, Zhang *et al.* 2021, She *et al.* 2021, Lu *et al.* 2021, Amar *et al.* 2018, Anirudh *et al.* 2020, Eltaher *et al.* 2018, Malikan *et al.* 2020, Faghidian 2016, 2017, Zenkour 2018, Heydari *et al.* 2018, Barretta *et al.* 2020, Jalaei and Civalek 2019, Zhang and She 2022, Zhang *et al.* 2022, Zhao *et al.* 2022, Ding and She 2021, Xu and She 2022). Due to the asymmetry of FG materials, the physical neutral surface concept is proposed as a new concept (Van-Loi *et al.* 2021, Babaei and Eslami 2020, Faleh *et al.* 2018, Attia and Mohamed 2020a, b, Zouatnia *et al.* 2017). For homogeneous materials, the physical neutral surface is at the same position as the geometric midplane of the structure. However, for FG materials, when the physical neutral surface concept is introduced, compared with the vibration equation based on the geometric midplane, the vibration equation based on the physical neutral surface concept does not have tension bending coupling effect, and the expression form of control equation and boundary condition is simpler, and the solution process is simpler. For example, with the help of the physical neutral surface concept, Babaei and Eslami (2021) used the nonlocal strain gradient theory to analyze the nonlinear bending behavior of FG shells. Considering the effect of hardening elastic foundations, Van-Loi *et al.* (2021) studied the bending behaviors of FG plates. Taking the consideration of pre/post-buckled state and modified couple stress models, Attia and Mohamed (2020a) discussed the vibrations of the bi-directional tapered beams consist of FG materials. Attia and Mohamed (2020b) also investigated thermal postbucking of a bi-directional tapered FG beam. Babaei *et al.* (2019) used non-classical theory to analyze the nonlinear vibration behavior of FG shells. Radic (2018) discussed FG plate with porosities using various theories. Arefi *et al.* (2018) analyzed the static bending of the FG plates using a new model. Kumar *et al.* (2018) studied the free vibration analysis of FG plates via dynamic stiffness technique. She *et al.* (2022) discussed the guided wave propagation of porous FG square plates incorporating thermal effects. She *et al.* (2022) discussed the wave propagation in an FG circular plate, however, they do not consider the thermal effects. Sun and Luo (2012) discussed the wave propagation and transient response of FG plates subjected to a point impact loads. Zhang and Zhou (2015) discussed the nonlinear bending of FG circular plates based on physical neutral surface concept. Based on a quasi-3D refined theory, Zenkour (2018) studied the vibration of FG sandwich plates with porosities resting on elastic foundation subjected to

*Corresponding author, Associate Professor
E-mail: sheguilin@cqu.edu.cn

ISSN: 2005-307X (Print), 2092-6219 (Online)

thermal environment. Zouatnia *et al.* (2017) applied a refined hyperbolic shear deformation theory to analyze the bending of FG beams via the neutral surface concept. Ahmadi *et al.* (2019) presented the nonlinear resonance of spiral stiffened FG cylindrical shells resting on damping and nonlinear elastic foundations. Akgöz and Civalek (2017) investigated the effects of thermal and shear deformation on free vibration of FG thick microbeams using various beam theories. Amar *et al.* (2018) used a new four-unknown refined theory to study the size-dependent bending and vibration analysis behaviors of FG micro-plate. Anirudh *et al.* (2020) presented the nonlinear bending of porous curved beams reinforced using the finite element approach. Arefi *et al.* (2018) used physical neutral surface concept to analyze FG piezoelectric plates. Ghayesh (Ghayesh 2018a, b, 2019) published some papers which discussed the nonlinear vibrations of axially FG beams using Euler, Timoshenko and higher-order shear deformation beam theories.

She *et al.* (2022) discussed the wave propagation in FG circular plates, however, they do not consider the thermal effects. This work is extended to the case of the wave propagation of FG circular plates in thermal environment. However, when the temperature rises, the whole structure or each part will expand with the increase of temperature. Therefore, it is necessary to consider the temperature effect. In this paper, we have simplified the temperature field, considered the uniform temperature field, studied the propagation characteristics of bending waves in the circular plate, we assumed that the elastic modulus and thermal expansion coefficient of FG materials are functions of temperature, and finally analyzed different factors on the propagation characteristics of bending waves in the circular plate, We find that the temperature field has a very significant effect on the bending wave of in FG circular plates.

2. Mathematical model

In order to facilitate the establishment of the mechanical model, we establish the coordinate system as shown in Fig. 1. In the following analysis, we assume that the elastic modulus $E(Z,T)$, density ρ (Z) and thermal expansion coefficient α (Z,T) of the FG circular plate only change continuously along the thickness direction of the plate, and Poisson's ratio μ=0.3. According to the relevant knowledge of material mechanics and elasticity, when we study the pure bending problem of FG structure, we will find that, the normal strain and normal stress of FG structure are equal to 0, and this plane is the so-called physical neutral surface, and the distance between the physical neutral surface and the geometric mid-plane is expressed by z_0, and (Zhang and Zhou 2015, She *et al.* 2022)

$$z_0 = \frac{\int_{-h/2}^{h/2} ZE_f(Z,T)dZ}{\int_{-h/2}^{h/2} E_f(Z,T)dZ} \tag{1}$$

From Eq. (1), we can see that for the structure symmetrical along the thickness direction, z_0= 0.

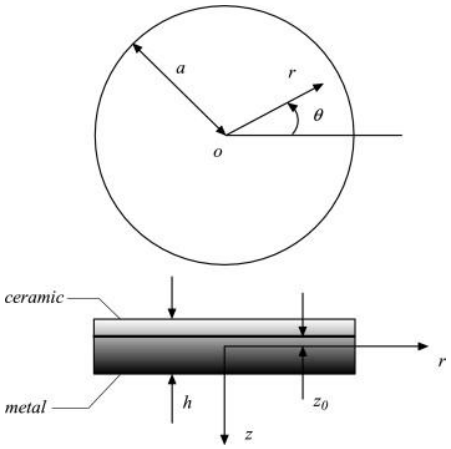

Fig. 1 An FG circular plate (Zhang and Zhou 2015)

In addition, we should note that z_0 is only related to the elastic modulus of FG material, and the elastic modulus is a function of temperature and thickness Z. In this paper, the FG material used is made of Si_3N_4 and SUS304, as shown in Table 1. From Table 1, we can see that the elastic modulus and thermal expansion coefficient of Si_3N_4 and SUS304 are closely related to temperature T, and have the following relationship expression (Reddy and Chin 1998, Ding *et al.* 2022)

$$P_m = P_0\left(P_{-1}T^{-1} + 1 + P_1T + P_2T^2 + P_3T^3\right) \tag{2}$$

In this paper, the classical power function is used to represent the elastic modulus $E(Z,T)$ and thermal expansion coefficient α (Z,T), and (She *et al*. 2017, 2022)

$$\begin{aligned} E(Z,T) &= \left[1-\left(\frac{2Z+h}{2h}\right)^N\right]E_m(T)+\left(\frac{2Z+h}{2h}\right)^N E_c(T) \\ &-\frac{\beta\left[E_m(T)+E_c(T)\right]}{2} \\ \alpha(Z,T) &= \left[1-\left(\frac{2Z+h}{2h}\right)^N\right]\alpha_m(T)+\left(\frac{2Z+h}{2h}\right)^N \alpha_c(T) \\ &-\frac{\beta\left[\alpha_m(T)+\alpha_c(T)\right]}{2} \end{aligned} \tag{3}$$

The effect of temperature on density $\rho(Z)$ can be ignored, and (She *et al*. 2017, 2022, Chen *et al.* 2022)

$$\rho(Z) = \left[1-\left(\frac{2Z+h}{2h}\right)^N\right]\rho_m+\left(\frac{2Z+h}{2h}\right)^N \rho_c - \frac{\beta\left[\rho_m+\rho_c\right]}{2} \tag{4}$$

in which, N is the functionally graded index, β is the porosity volume fraction. In addition, in this paper, for the convenience of calculation, Poisson's ratio μ=0.3.

At present, there are many literatures neglected the influence of porosity volume fraction on material properties. In that case, Eqs. (3) and (4) become

$$\begin{aligned} E(Z,T) &= \left[1-\left(\frac{2Z+h}{2h}\right)^N\right]E_m(T)+\left(\frac{2Z+h}{2h}\right)^N E_c(T) \\ \alpha(Z,T) &= \left[1-\left(\frac{2Z+h}{2h}\right)^N\right]\alpha_m(T)+\left(\frac{2Z+h}{2h}\right)^N \alpha_c(T) \end{aligned} \tag{5}$$

Table 1 Material properties of Si_3N_4 and SUS304, from Reddy and Chin (1998)

Materials	Proprieties	P_0	P_{-1}	P_1	P_2	P_3
Si_3N_4	E_c(Pa)	348.43e+9	0.0	-3.070e-4	2.160e-7	-8.964e-11
	α_c (1/K)	5.8723e-6	0.0	9.095e-4	0.0	0.0
	ρ_c(Kg/m^3)	2370	0.0	0.0	0.0	0.0
SUS304	E_m(Pa)	201.04e+9	0.0	3.079e-4	-6.543e-7	0.0
	α_m (1/K)	12.33e-6	0.0	8.086e-4	0.0	0.0
	ρ_m(Kg/m^3)	8166	0.0	0.0	0.0	0.0

$$\rho(Z)=\left[1-\left(\frac{2Z+h}{2h}\right)^N\right]\rho_m+\left(\frac{2Z+h}{2h}\right)^N\rho_c \tag{6}$$

In the previous article of the authors, we studied the influence of temperature change ΔT and functionally graded index N on z_0, as shown in Fig. 2. From the figure, we can see that with the increase of the functionally graded index N, z_0 is an increasing function of N within a certain interval, followed by a decreasing function of N. In addition, the greater the temperature T, the greater the z_0 is, which shows that the position of the neutral axis z_0 is significantly affected by the functionally graded index N and temperature change ΔT, which cannot be ignored in the process of analysis and modeling.

Based on the physical neutral surface concept and first-order shear deformation plate theory, the displacement field has the following forms (Zhang and Zhou 2015, She *et al*. 2022)

$$\begin{aligned} U_R(R,Z,t^{'})&=U_0(R,t^{'})+(Z-z_0)\varphi(R,t^{'})\\ U_z(R,Z,t^{'})&=W(R,t^{'}) \end{aligned} \tag{7}$$

Where, $U_R(R,Z,t^{'})$ and $U_z(R,Z,t^{'})$ are the radial displacement and transverse displacement of the circular plate, $W(R,t^{'})$ is the deflection of the plate, φ stands for the rotation along the R direction.

According to the linear geometric relationship, the expression of strain can be obtained (She *et al*. 2022)

$$\begin{aligned} \varepsilon_R&=\frac{\partial U_R}{\partial R}=\frac{\partial U_0}{\partial R}+(Z-z_0)\frac{\partial\varphi}{\partial R}\\ &=\frac{\partial U_0}{\partial R}+\left(Z-\frac{\int_{-h/2}^{h/2}ZE(Z,T)dZ}{\int_{-h/2}^{h/2}E_f(Z,T)dZ}\right)\frac{\partial\varphi}{\partial R} \end{aligned} \tag{8}$$

$$\begin{aligned} \varepsilon_\theta&=\frac{U_R}{R}=\frac{U_0}{R}+(Z-z_0)\frac{\varphi}{R}\\ &=\frac{U_0}{R}+\left(Z-\frac{\int_{-h/2}^{h/2}ZE(Z,T)dZ}{\int_{-h/2}^{h/2}E(Z,T)dZ}\right)\frac{\varphi}{R}\\ \varepsilon_{RZ}&=\frac{\partial U_R}{\partial Z}+\frac{\partial U_Z}{\partial R}=\varphi+\frac{\partial W}{\partial R}. \end{aligned}$$

Considering thermal effect, the relationship between stresses and strains are

$$\begin{aligned} \begin{Bmatrix}\sigma_R^{'}\\ \sigma_\theta^{'}\\ \sigma_{RZ}^{'}\end{Bmatrix}&=\begin{bmatrix}\frac{E(Z,T)}{1-\nu^2}&\frac{\nu E(Z,T)}{1-\nu^2}&0\\ \frac{\nu E(Z,T)}{1-\nu^2}&\frac{E(Z,T)}{1-\nu^2}&0\\ 0&0&\frac{\gamma^2E(Z,T)}{2(1+\nu)}\end{bmatrix}\begin{Bmatrix}\varepsilon_R\\ \varepsilon_\theta\\ \varepsilon_{RZ}\end{Bmatrix}\\ &-\frac{E(Z,T)}{1-\nu}\alpha(z,T)\Delta T\\ &=\begin{bmatrix}\frac{E(Z,T)}{1-\nu^2}&\frac{\nu E(Z,T)}{1-\nu^2}&0\\ \frac{\nu E(Z,T)}{1-\nu^2}&\frac{E(Z,T)}{1-\nu^2}&0\\ 0&0&\frac{\gamma^2E(Z,T)}{2(1+\nu)}\end{bmatrix}\\ &\times\begin{Bmatrix}\frac{\partial U_0}{\partial R}+\left(Z-\frac{\int_{-h/2}^{h/2}ZE(Z,T)dZ}{\int_{-h/2}^{h/2}E(Z,T)dZ}\right)\frac{\partial\varphi}{\partial R}\\ \frac{U_0}{R}+\left(Z-\frac{\int_{-h/2}^{h/2}ZE(Z,T)dZ}{\int_{-h/2}^{h/2}E(Z,T)dZ}\right)\frac{\varphi}{R}\\ \varphi+\frac{\partial W}{\partial R}\end{Bmatrix}-\frac{E(Z,T)}{1-\nu}\alpha(z,T)\Delta T \end{aligned} \tag{9}$$

Herein, $\gamma^2=5/6$ is the shear correction factor.

These internal forces have the following definitions

$$\begin{aligned} &N_R=\int_{-\frac{h}{2}}^{\frac{h}{2}}\sigma_R^{'}dZ,N_\theta=\int_{-\frac{h}{2}}^{\frac{h}{2}}\sigma_\theta^{'}dZ,Q_R=\int_{-\frac{h}{2}}^{\frac{h}{2}}\sigma_{RZ}^{'}dZ,\\ &M_R=\int_{-\frac{h}{2}}^{\frac{h}{2}}(Z-z_0)\sigma_R^{'}dZ,M_\theta=\int_{-\frac{h}{2}}^{\frac{h}{2}}(Z-z_0)\sigma_\theta^{'}dZ. \end{aligned} \tag{10}$$

With the help of Eqs. (6)-(9), Eq. (10) becomes

$$\begin{aligned} N_R&=\int_{-\frac{h}{2}}^{\frac{h}{2}}\begin{bmatrix}\frac{E(Z,T)}{1-\nu^2}\varepsilon_R+\frac{\nu E(Z,T)}{1-\nu^2}\varepsilon_\theta dZ\\ -\frac{E(Z,T)}{1-\nu}\alpha(z,T)\Delta T\end{bmatrix}dZ\\ &=\int_{-\frac{h}{2}}^{\frac{h}{2}}\begin{bmatrix}\frac{E(Z,T)}{1-\nu^2}\left(\frac{\partial U_0}{\partial R}+(Z-z_0)\frac{\partial\varphi}{\partial R}\right)\\ +\frac{\nu E(Z,T)}{1-\nu^2}\left(\frac{U_0}{R}+(Z-z_0)\frac{\varphi}{R}\right)dZ\\ -\frac{E(Z,T)}{1-\nu}\alpha(z,T)\Delta T\end{bmatrix}dZ \end{aligned} \tag{11}$$

$$N_\theta = \int_{-\frac{h}{2}}^{\frac{h}{2}} \left[\begin{array}{l} \dfrac{\nu E(Z,T)}{1-\nu^2}\varepsilon_R + \dfrac{E(Z,T)}{1-\nu^2}\varepsilon_\theta dZ \\ -\dfrac{E(Z,T)}{1\text{-}\nu}\alpha(z,T)\Delta T \end{array} \right] dZ$$

$$= \int_{-\frac{h}{2}}^{\frac{h}{2}} \left[\begin{array}{l} \dfrac{\nu E(Z,T)}{1-\nu^2}\left(\dfrac{\partial U_0}{\partial R} + (Z-z_0)\dfrac{\partial \varphi}{\partial R}\right) \\ +\dfrac{E(Z,T)}{1-\nu^2}\left(\dfrac{U_0}{R} + (Z-z_0)\dfrac{\varphi}{R}\right) dZ \\ -\dfrac{E(Z,T)}{1\text{-}\nu}\alpha(z,T)\Delta T \end{array} \right] dZ \tag{12}$$

$$= A_{12}\frac{\partial U_0}{\partial R} + A_{22}\frac{U_0}{R} - N^T$$

$$M_R = \int_{-\frac{h}{2}}^{\frac{h}{2}} (Z-z_0) \left[\begin{array}{l} \dfrac{E(Z,T)}{1-\nu^2}\varepsilon_R + \dfrac{\nu E(Z,T)}{1-\nu^2}\varepsilon_\theta dZ \\ -\dfrac{E(Z,T)}{1\text{-}\nu}\alpha(z,T)\Delta T \end{array} \right] dZ$$

$$= \int_{-\frac{h}{2}}^{\frac{h}{2}} (Z-z_0) \left[\begin{array}{l} \dfrac{E(Z,T)}{1-\nu^2}\left(\dfrac{\partial U_0}{\partial R} + (Z-z_0)\dfrac{\partial \varphi}{\partial R}\right) \\ +\dfrac{\nu E(Z,T)}{1-\nu^2}\left(\dfrac{U_0}{R} + (Z-z_0)\dfrac{\varphi}{R}\right) dZ \\ -\dfrac{E(Z,T)}{1\text{-}\nu}\alpha(z,T)\Delta T \end{array} \right] dZ \tag{13}$$

$$= D_{11}\frac{\partial \varphi}{\partial R} + D_{12}\frac{\varphi}{R} - M^T$$

$$M_\theta = \int_{-\frac{h}{2}}^{\frac{h}{2}} (Z-z_0) \left[\begin{array}{l} \dfrac{\nu E(Z,T)}{1-\nu^2}\varepsilon_R + \dfrac{E(Z,T)}{1-\nu^2}\varepsilon_\theta dZ \\ -\dfrac{E(Z,T)}{1\text{-}\nu}\alpha(z,T)\Delta T \end{array} \right] dZ$$

$$= \int_{-\frac{h}{2}}^{\frac{h}{2}} (Z-z_0) \left[\begin{array}{l} \dfrac{\nu E(Z,T)}{1-\nu^2}\left(\dfrac{\partial U_0}{\partial R} + (Z-z_0)\dfrac{\partial \varphi}{\partial R}\right) \\ +\dfrac{E(Z,T)}{1-\nu^2}\left(\dfrac{U_0}{R} + (Z-z_0)\dfrac{\varphi}{R}\right) dZ \\ -\dfrac{E(Z,T)}{1\text{-}\nu}\alpha(z,T)\Delta T \end{array} \right] dZ \tag{14}$$

$$= D_{12}\frac{\partial \varphi}{\partial R} + D_{22}\frac{\varphi}{R} - M^T$$

$$Q_R = \int_{-\frac{h}{2}}^{\frac{h}{2}} \frac{\gamma^2 E(Z,T)}{2(1+\nu)}\left(\varphi + \frac{\partial W}{\partial R}\right) dZ \tag{15}$$

After arrangement, one has

$$\begin{aligned} &N_R = A_{11}\frac{\partial U_0}{\partial R} + A_{12}\frac{U_0}{R} - N^T, N_\theta = A_{12}\frac{\partial U_0}{\partial R} + A_{22}\frac{U_0}{R} - N^T, \\ &M_R = D_{11}\frac{\partial \varphi}{\partial R} + D_{12}\frac{\varphi}{R} - M^T, M_\theta = D_{12}\frac{\partial \varphi}{\partial R} + D_{22}\frac{\varphi}{R} - M^T, \\ &Q_R = A_{55}(\varphi + \frac{\partial W}{\partial R}). \end{aligned} \tag{16}$$

in which

$$A_{11} = A_{22} = \int_{-\frac{h}{2}}^{\frac{h}{2}} \frac{E(Z,T)}{1-\nu^2}\,\mathrm{d}Z \tag{17}$$

$$A_{12} = \int_{-\frac{h}{2}}^{\frac{h}{2}} \frac{\nu E(Z,T)}{1-\nu^2}\,\mathrm{d}Z \tag{18}$$

$$A_{55} = \int_{-\frac{h}{2}}^{\frac{h}{2}} \frac{\gamma^2 E(Z,T)}{2(1+\nu)}\,\mathrm{d}Z \tag{19}$$

$$D_{12} = \int_{-\frac{h}{2}}^{\frac{h}{2}} (Z-z_0)^2 \frac{\nu E(Z,T)}{1-\nu^2}\,\mathrm{d}Z \tag{20}$$

$$D_{11} = D_{22} = \int_{-\frac{h}{2}}^{\frac{h}{2}} (Z-z_0)^2 \frac{E(Z,T)}{1-\nu^2}\,\mathrm{d}Z \tag{21}$$

$$N^T = \int_{-h/2}^{h/2} E(Z,T)\alpha(Z,T)\Delta T dZ \tag{22}$$

$$M^T = \int_{-h/2}^{h/2} (Z-z_0)E(Z,T)\alpha(Z,T)\Delta T dZ \tag{23}$$

Using Hamilton variational principle, we can derive the motion equation of FG circular plate as follows

$$\begin{aligned} &-N_\theta + \frac{\partial}{\partial R}(RN_R) = R(I_0\ddot{U}_0 + I_1\ddot{\varphi}) \\ &-M_\theta - RQ_R + \frac{\partial}{\partial R}(RM_R) = R(I_1\ddot{U}_0 + I_2\ddot{\varphi}) \\ &\frac{\partial}{\partial R}(RQ_R) = RI_0\ddot{W} \end{aligned} \tag{24}$$

where

$$I_0 = \int_{-\frac{h}{2}}^{\frac{h}{2}} \rho(Z)\,\mathrm{d}Z \tag{25}$$

$$I_1 = \int_{-\frac{h}{2}}^{\frac{h}{2}} \rho(Z)(Z-z_0)\,\mathrm{d}Z \tag{26}$$

$$I_2 = \int_{-\frac{h}{2}}^{\frac{h}{2}} \rho(Z)(Z-z_0)^2\,\mathrm{d}Z \tag{27}$$

Using Eq. (16), Eq. (24) becomes

$$\begin{aligned} &\frac{1}{R}\left[\frac{\partial}{\partial R}(RN_R) - N_\theta\right] = A_{11}(\frac{1}{R}\frac{\partial}{\partial R}(R\frac{\partial}{\partial R}) - \frac{1}{R^2})U_0 \\ &= -\left(A_{12}\frac{\partial U_0}{\partial R} + A_{22}\frac{U_0}{R}\right) + N^T \\ &+ \frac{\partial}{\partial R}\left[R\left(A_{11}\frac{\partial U_0}{\partial R} + A_{12}\frac{U_0}{R}\right)\right] \\ &= A_{11}\left(\frac{1}{R}\frac{\partial}{\partial R}(R\frac{\partial U_0}{\partial R})\right) + A_{12}\frac{\partial U_0}{\partial R} - A_{12}\frac{\partial U_0}{\partial R} \\ &- A_{22}\frac{1}{R^2}U_0 + N^T = A_{11}\left(\frac{1}{R}\frac{\partial}{\partial R}(R\frac{\partial U_0}{\partial R})\right) - \frac{A_{11}}{R^2}U_0 + N^T \\ &= A_{11}(\frac{1}{R}\frac{\partial}{\partial R}(R\frac{\partial}{\partial R}) - \frac{1}{R^2})U_0 + N^T = I_0\ddot{U}_0 + I_1\ddot{\varphi}, \\ &\frac{1}{R}\left[\frac{\partial}{\partial R}(RM_R) - M_\theta - RQ_R\right] \\ &= \frac{1}{R}\left[\begin{array}{l} \dfrac{\partial}{\partial R}\left[R(D_{11}\dfrac{\partial \varphi}{\partial R} + D_{12}\dfrac{\varphi}{R})\right] \\ -(D_{12}\dfrac{\partial \varphi}{\partial R} + D_{22}\dfrac{\varphi}{R}) - RA_{55}(\varphi + \dfrac{\partial W}{\partial R}) \end{array}\right] + M^T \\ &= D_{11}(\frac{1}{R}\frac{\partial}{\partial R}(R\frac{\partial}{\partial R}) - \frac{1}{R^2})\varphi - A_{55}(\varphi + \frac{\partial W}{\partial R}) + M^T \\ &= I_1\ddot{U}_0 + I_2\ddot{\varphi}, \\ &\frac{1}{R}\frac{\partial}{\partial R}(RQ_R) = \frac{1}{R}\frac{\partial}{\partial R}(RA_{55}(\varphi + \frac{\partial W}{\partial R})) \\ &= A_{55}\frac{1}{R}\frac{\partial}{\partial R}[R(\varphi + \frac{\partial W}{\partial R})] = I_0\ddot{W} \end{aligned} \tag{28}$$

After arrangement, we can obtain

$$\begin{aligned} &A_{11}(\frac{1}{R}\frac{\partial}{\partial R}(R\frac{\partial}{\partial R})-\frac{1}{R^2})U_0+N^T=I_0\ddot{U}_0+I_1\ddot{\varphi}\\ &D_{11}(\frac{1}{R}\frac{\partial}{\partial R}(R\frac{\partial}{\partial R})-\frac{1}{R^2})\varphi-A_{55}(\varphi+\frac{\partial W}{\partial R})+M^T\\ &\quad=I_1\ddot{U}_0+I_2\ddot{\varphi}\\ &A_{55}\frac{1}{R}\frac{\partial}{\partial R}[R(\varphi+\frac{\partial W}{\partial R})]=I_0\ddot{W} \end{aligned} \tag{29}$$

Considering the following initial conditions (Sun and Luo 2012, She *et al*. 2022)

$$\boldsymbol{U}\big|_{t=0}=0,\qquad \dot{\boldsymbol{U}}\big|_{t=0}=0 \tag{30}$$

Herein， $\boldsymbol{U}=[u,\varphi,w]^{\mathrm{T}}$, Using the Laplace integral transformation, the first order Hankel integral transformation and the zero order Hankel integral transformation, the expression of phase velocity, group velocity for the bending wave can be found.

3. Numerical analysis

Fig. 3 shows the influence of the functionally graded index N on the propagation characteristics of bending waves in an FG circular plate. During calculation, $\Delta T=0, \beta=0$. Through comparison, the results of this study are completely consistent with She *et al.* (2022), which verifies the correctness of this study.

In the following analysis, the adopted materials are Si_3N_4 and SUS304, as shown in Table 1.

Because the difference between the present paper and the previous work is that the effect of temperature changes ΔT is taken into account. So, it is important to study the effect of temperature changes ΔT in the following analysis. In Fig. 4, we studied the effect of temperature changes ΔT=(0,400K,600K,800K) on the phase- and group-velocity of bending waves. It can be seen that the phase velocity is a monotone increasing function of wave number,

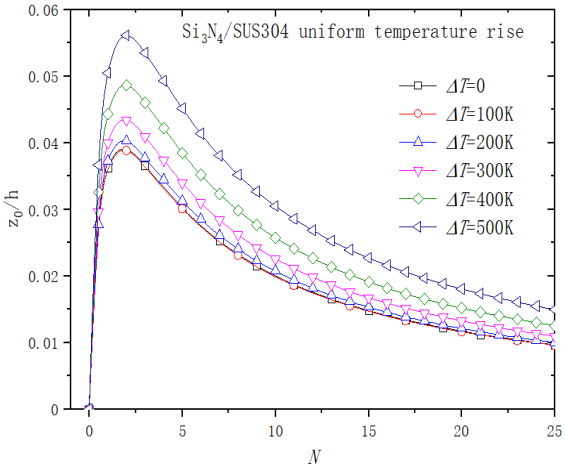

Fig. 2 Effect of temperature and functionally graded index N on the value z_0 (She *et al.* 2017)

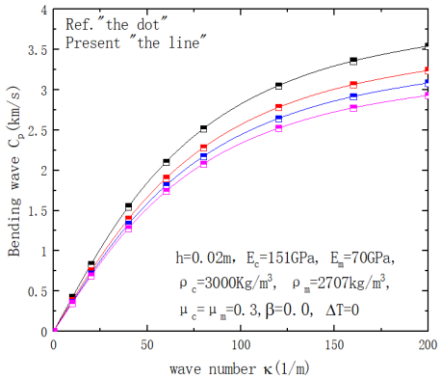

Fig. 3 Comparison of wave propagation of FG circular pl ate (ΔT=0, $\beta=0$) with She *et al*. (2022)

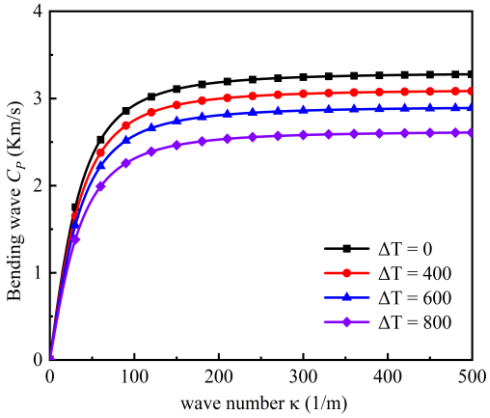

(a) Phase velocity

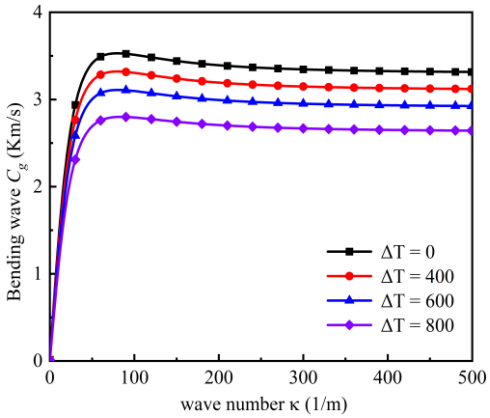

(b) Group velocity

Fig. 4 Effect of temperature changes $\Delta T(K)$ on wave propagation of FG circular plates (N=3, β=0.1)

whiles the group velocity is not a monotone increasing function of wave number. In addition, we can also see that the phase and group velocity decrease correspondingly as the temperature rises. This is because the increase of temperature will reduce the elastic modulus and density of FG circular plate, thus reducing the bending stiffness of the circular plate, thus reducing the wave propagation velocity. Therefore, when FG material is at high temperature, the effect of temperature on wave propagation cannot be ignored. If the effect of temperature is ignored, it will inevitably lead to wrong results.

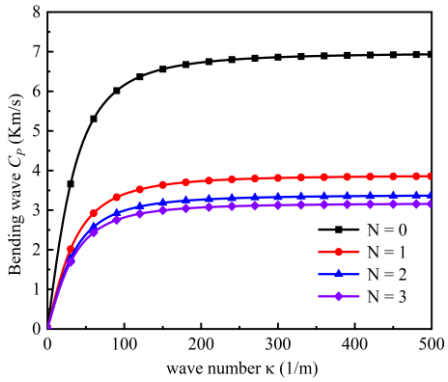

(a) Phase velocity

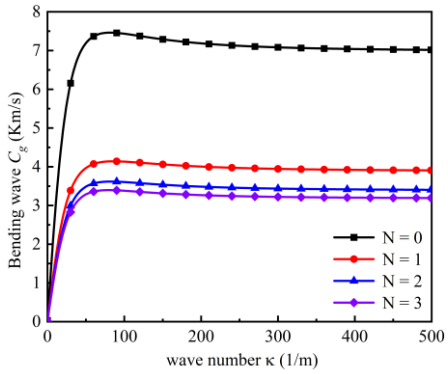

(b) Group velocity

Fig. 5 Effect of functionally graded index N on wave propagation of FG circular plates (ΔT=300K, β=0.1)

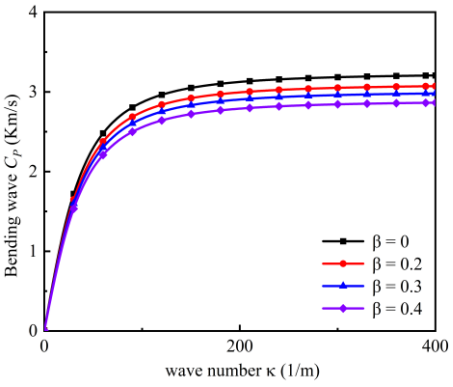

(a) Phase velocity

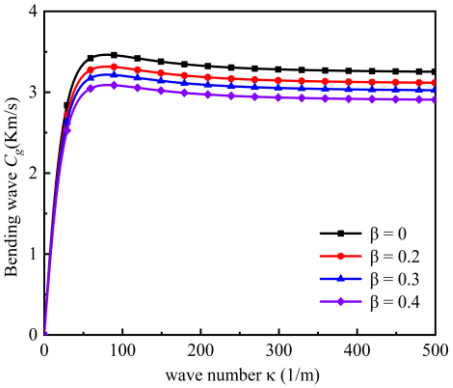

(b) Group velocity

Fig. 6 Effect of porosity volume fraction β on wave propagation of FG circular plates (ΔT=300K, N=3)

In Fig. 5, we studied the influence of the functionally graded index N on the phase velocity and group velocity of wave propagation. From the figure, we can see that the functionally graded index N has a very significant impact on velocities. With the continuous increase of N, the propagation velocity of the phase velocity and group velocity decreases significantly. This is because, with the increasing of N, the volume fraction of SUS304 contained in FG material is increasing, and the volume fraction of Si_3N_4 is decreasing, while the elastic modulus and Poisson's ratio of SUS304 are smaller than those of Si_3N_4. Therefore, with the increasing of N, the stiffness of the circular plate will decrease. So, like the effect of temperature rise, in the process of wave propagation, both phase- and group-velocity decrease.

In Fig. 6, we studied the effect of porosity volume fraction β on bending wave, it can be seen that β has a significant impact on the wave propagation, with the increasing of porosity volume fraction β, the propagation velocity of phase velocity and group velocity decreases significantly. This is because, with the constant increase of porosity volume fraction β, the more pores in FG material, the stiffness of the circular plate will decrease. Therefore, like the effect of temperature rise, the velocity will decrease in the process of wave propagation.

4. Conclusions

Considering temperature changes and porosity, based on the physical neutral surface concept, we studied the propagation characteristics of bending waves in FG circular plates. The following conclusions can be drawn for this paper:

(1) The phase velocity is a monotone increasing function of wave number, whiles the group velocity is not a monotone increasing function of wave number.
(2) The phase- and group- velocity decrease as the temperature rises. This is because the increase of temperature will reduce the bending stiffness of the circular plate.
(3) With the continuous increase of N, the wave velocity decreases significantly.
(4) With the increase of porosity volume fraction β, the propagation velocity decreases significantly.

Acknowledgments

The authors acknowledge this work is supported by the Hunan Provincial Innovation Foundation for Postgraduate (CX20190258).

References

Ahmadi, H. (2019), "Nonlinear primary resonance of imperfect spiral stiffened functionally graded cylindrical shells surrounded by damping and nonlinear elastic foundation", *Eng. Comput.*, **35**, 1491-1505. http://doi.org/10.1007/s00366-018-0679-2.
Akgöz, B. and Civalek, O. (2017), "Effects of thermal and shear

deformation on vibration response of functionally graded thick composite microbeams", *Compos. Part B.-Eng*., **129**, 77-87. https://doi.org/10.1016/j.compositesb.2017.07.024.

Amar, L.H.H., Kaci, A., Yeghnem, R. and Tounsi, A. (2018), "Anew four-unknown refined theory based on modified couple stress theory for size-dependent bending and vibration analysisof functionally graded micro-plate", *Steel Compos. Struct.,* **26**(1), 89-102. https://doi.org/10.12989/scs.2018.26.1.089.

Anirudh, B, Ben Zineb, T., Polit, O., Ganapathi, M. and Prateek, G. (2020), "Nonlinear bending of porous curved beams reinforced by functionally graded nanocomposite graphene platelets applying an efficient shear flexible finite element approach", *Int. J. Nonlin. Mech.*, **119**, 103346. https://doi.org/10.1016/j.ijnonlinmec.2019.103346.

Arefi, M., Bidgoli, E.M.R., Dimitri, R., Bacciocchi, M. and Tornabene, F. (2018), "Application of sinusoidal shear deformation theory and physical neutral surface to analysis of functionally graded piezoelectric plate", *Compos. Part B.-Eng*., **151**, 35-50. http://doi.org/10.1016/j.compositesb.2018.05.050.

Attia, M.A. and Mohamed, S.A. (2020a), "Thermal vibration characteristics of pre/post-buckled bi-directional functionally graded tapered microbeams based on modified couple stress Reddy beam theory", *Eng. Comput*., https://doi.org/10.1007/s00366-020-01188-4.

Attia, M.A. and Mohamed, S.A. (2020b), "Nonlinear thermal buckling and postbuckling analysis of bidirectional functionally graded tapered microbeams based on Reddy beam theory", *Eng. Comput.*, https://doi.org/10.1007/s00366-020-01080-1.

Babaei, H. and Eslami, M.R.(2021), "Nonlinear analysis of thermal-mechanical coupling bending of FGP infinite length cylindrical panels based on PNS and NSGT", *Appl. Math. Model*., **91**, 1061-1080. https://doi.org/10.1016/j.apm.2020.10.004.

Babaei, H., Kiani, Y. and Eslami, M.R. (2019), "Large amplitude free vibrations of long FGM cylindrical panels on nonlinear elastic foundation based on physical neutral surface", *Compos. Struct*., **220**, 888-898. https://doi.org/10.1016/j.compstruct.2019.03.064.

Barretta, R. Ali Faghidian, S. and Marotti de Sciarra, F., Penna, R., and Pinnola F.P. (2020), "On torsion of nonlocal Lam strain gradient FG elastic beams", *Compos. Struct.*, **233**, 111550. https://doi.org/10.1016/j.compstruct.2019.111550.

Chen, X., Zhao, J.L., She, G.L., Jing, Y., Luo, J. and Pu, H.Y. (2022), "On wave propagation of functionally graded CNT strengthened fluid-conveying pipe in thermal environment", *Eur. Phys. J. Plus*, **137**(10), 1158. https://doi.org/10.1140/epjp/s13360-022-03234-0.

Dehrouyeh-Semnani, A.M., Dehdashti, E., Yazdi, M. and Nikkhah-Bahrami, M. (2019), "Nonlinear thermo-resonant behavior of fluid-conveying FG pipes", *Int. J. Eng. Sci*., **144**, 103141. http://dx.doi.org/10.1016/j.ijengsci.2019.103141.

Ding, H.X. and She, G.L. (2021), "A higher-order beam model for the snap-buckling analysis of FG pipes conveying fluid", *Struct. Eng. Mech*., **80**(1), 63-72. https://doi.org/10.12989/sem.2021.80.1.063.

Ding, H.X., She, G.L. and Zhang, Y.W. (2022), "Nonlinear buckling and resonances of functionally graded fluid-conveying pipes with initial geometric imperfection", *Eur. Phys. J. Plus*, 137:1329. https://doi.org/10.1140/epjp/s13360-022-03570-1.

Eltaher, M.A., Fouda, N., El-Midany, T. and Sadoun, A.M.(2018), "Modified porosity model in analysis of functionally graded porous nanobeams", *J. Brazil. Soc. Mech. Sci. Eng*., **40**(3), 141. https://doi.org/10.1007/s40430-018-1065-0.

Faghidian, S.A. (2016), "Unified formulation of the stress field of saint-Venant's flexure problem for symmetric cross-sections", *Int. J. Mech. Sci*., **111-112**, 65-72. https://doi.org/10.1016/j.ijmecsci.2016.04.003.

Faghidian, S.A. (2017), "Unified formulations of the shear coefficients in timoshenko beam theory", *J. Eng. Mech.*, **143**(9), 06017013. http://doi.org/10.1061/(ASCE)EM.1943-7889.0001297.

Faleh, N.M., Ahmed, R.A. and Fenjan, R.M. (2018), "On vibrations of porous FG nanoshells", *Int. J. Eng. Sci*., **133**, 1-14. https://doi.org/10.1016/j.ijengsci.2018.08.007.

Ghayesh, M.H. (2018a), "Nonlinear vibrations of axially functionally graded timoshenko tapered beams", *J. Comput. Nonlinear. Dynam*, **13**(4), 041002. https://doi.org/10.1115/1.4039191.

Ghayesh, M.H. (2018b), "Mechanics of tapered AFG shear-deformable microbeams", *Microsyst. Technol*., **24**, 1743-1754. https://doi.org/10.1007/s00542-018-3764-y.

Ghayesh, M.H. (2019), "Nonlinear oscillations of FG cantilevers", *Appl. Acoust*, **145**, 393-398. https://doi.org/10.1016/j.apacoust.2018.08.014.

Heydari, A. (2018), "Exact vibration and buckling analyses ofarbitrary gradation of nano-higher order rectangular beam", *Steel Compos. Struct.*, **28**(5), 589-606. https://doi.org/10.12989/scs.2018.28.5.589.

Jalaei, M.H. and Civalek, Ö. (2019), "On dynamic instability of magnetically embedded viscoelastic porous FG nanobeam", *Int. J. Eng. Sci.*, **143**, 14-32. https://doi.org/10.1016/j.ijengsci.2019.06.013.

Kumar, S., Ranjan, V. and Jana, P. (2018), "Free vibration analysis of thin functionally graded rectangular plates using the dynamic stiffness method", *Compos. Struct*., **197**, 39-53. http://doi.org/10.1016/j.compstruct.2018.04.085.

Lu, L., She, G.L. and Guo, X. (2021), "Size-dependent postbuckling analysis of graphene reinforced composite microtubes with geometrical imperfection", *Int. J. Mech. Sci*., 199, 106428. https://doi.org/10.1016/j.ijmecsci.2021.106428.

Malikan, M., Krasheninnikov, M. and Eremeyev, V.A. (2020), "Torsional stability capacity of a nano-composite shell based on a nonlocal strain gradient shell model under a three-dimensional magnetic field", *Int. J. Eng. Sci*., **148**, 103234. https://doi.org/10.1016/j.ijengsci.2019.103210.

Nguyen, V.L., Tran, M.T., Nguyen, V.L. and Le, Q.H. (2021), "Static behaviour of functionally graded plates resting on elastic foundations using neutral surface concept", Archive of mechanical engineering, 68(1), 5-22.https://doi.org/10.24425/ame.2020.131706

Radic, N. (2018), "On buckling of porous double-layered FG nanoplates in the Pasternak elastic foundation based on nonlocal strain gradient elasticity", *Compos. Part B.-Eng*., **153**, 465-479. https://doi.org/10.1016/j.compositesb.2018.09.014.

Reddy, J.N. and Chin, C.D. (1998), "Thermomechanical analysis of functionally graded cylinders and plates", *J. Therm. Stresses*, **21**(6), 593-626. https://doi.org/10.1080/01495739808956165.

She, G.L. (2021), "Guided wave propagation of porous functionally graded plates: The effect of thermal loadings", *J. Therm. Stresses*, **44**(10), 1289-1305. https://doi.org/10.1080/01495739.2021.1974323.

She, G.L., Ding, H.X. and Zhang, Y.W. (2022), "Wave propagation in a FG circular plate via the physical neutral surface concept", *Struct. Eng. Mech*., **82**(2), 225-232. https://doi.org/10.12989/sem.2022.82.2.225.

She, G.L., Liu, H.B. and Karami, B. (2021), "Resonance analysis of composite curved microbeams reinforced with graphenenanoplatelets", *Thin Wall. Struct*., **160**, 107407. https://doi.org/10.1016/j.tws.2020.107407.

She, G.L., Yuan, F.G. and Ren, Y.R. (2017), "Thermal buckling and postbuckling analysis of piezoelectric FGM beams based on high-order shear deformation theory", *J. Therm. Stresses*, **40**(6), 783-797. https://doi.org/10.1080/01495739.2016.1261009.

Sun, D. and Luo, S.N. (2012), "Wave propagation and transient response of a functionally graded material plate under a point impact load in thermal environments", *Appl. Math. Model*., **36**(1), 444-462. https://doi.org/10.1016/j.apm.2011.07.023.

Xu, J.Q. and She, G.L. (2022), "Thermal post-buckling analysis of porous functionally graded pipes with initial geometric imperfection", *Geomech. Eng*., **31**(3), 329-337. https://doi.org/10.12989/gae.2022.31.3.329.

Zenkour, A.M. (2018), "A quasi-3D refined theory for functionallygraded single-layered and sandwich plates with porosities", *Compos. Struct.*, **201**, 38-48. https://doi.org/10.1016/j.compstruct.2018.05.147.

Zenkour, A.M. and Radwan, A.F. (2019), "Bending response of FG plates resting on elastic foundations in hygrothermalenvironment with porosities", *Compos. Struct.*,**213**, 133-143.https://doi.org/10.1016/j.compstruct.2019.01.065

Zhang, D.G. and Zhou, H.M. (2015), "Nonlinear bending analysis of FGM circular plates based on physical neutral surface and higher-order shear deformation theory", *Aerosp. Sci. Technol*., **41**, 90-98.https://doi.org/10.1016/j.ast.2014.12.016.

Zhang, Y.W. and She, G.L. (2022), "Wave propagation and vibration of FG pipes conveying hot fluid", *Steel Compos. Struct*., **42**(3), 397-405. https://doi.org/10.12989/scs.2022.42.3.397.

Zhang, Y.W., Ding, H.X. and She, G.L. (2022), "Snap-buckling and resonance of functionally graded graphene reinforced composites curved beams resting on elastic foundations in thermal environment", *J. Therm. Stresses*, **45**(12), 1029-1042. https://doi.org/10.1080/01495739.2022.2125137.

Zhang, Y.Y., Wang, X.Y., Zhang, X., Shen, H.M. and She, G.L. (2021), "On snap-buckling of FG-CNTR curved nanobeams considering surface effects", *Steel Compos. Struct*., **38**(3), 293-304. https://doi.org/10.12989/scs.2021.38.3.293.

Zhao, J.L., Chen, X., She, G.L., Jing, Y., Bai, R.Q., Yi, J., Pu, H.Y. and Luo, J. (2022), "Vibration characteristics of functionally graded carbon nanotube-reinforced composite double-beams in thermal environments", *Steel Compos. Struct*. **43**(6), 797-808. http://dx.doi.org/10.12989/scs.2022.43.6.797.

Zouatnia, N., Hadji, L. and Kassoul, A. (2017), "A refined hyperbolic shear deformation theory for bending of functionally graded beams based on neutral surface position", *Struct. Eng. Sci*., **63**(5), 683-689. http://doi.org/10.12989/sem.2017.63.5.683.